Atmospheric Environment 170 (2017) 169–183

Contents lists available at ScienceDirect

Atmospheric Environment

journal homepage: www.elsevier.com/locate/atmosenv

Aerosol particle mixing state, refractory particle number size distributions and emission factors in a polluted urban environment: Case study of Metro Manila, Philippines

Simonas Kecorius [a, *], Leizel Madueño [d], Edgar Vallar [b], Honey Alas [a, d, f], Grace Betito [d, f], Wolfram Birmili [a, e], Maria Obiminda Cambaliza [d, f], Grethyl Catipay [d, f], Mylene Gonzaga-Cayetano [c], Maria Cecilia Galvez [b], Genie Lorenzo [f], Thomas Müller [a], James B. Simpas [d, f], Everlyn Gayle Tamayo [b, c], Alfred Wiedensohler [a]

[a] Leibniz-Institute for Tropospheric Research, Permoserstr. 15, Leipzig, Germany
[b] ARCHERS, CENSER, De La Salle University, Manila, Philippines
[c] Institute of Environmental Science and Meteorology, University of the Philippines Diliman, Philippines
[d] Department of Physics, Ateneo de Manila University, Quezon City, Philippines
[e] Federal Environment Agency, Berlin, Germany
[f] Manila Observatory, Quezon City, Philippines

HIGHLIGHTS

- Aerosol particles in urban Metro Manila are mixed exclusively externally.
- Urban aerosol is dominated by refractory ultrafine particles.
- Soot emission from *Jeepneys* contributes up to 94% of total urban soot mass.
- In developing countries PM_{10} is not sufficient metric to evaluate air quality.

GRAPHICAL ABSTRACT

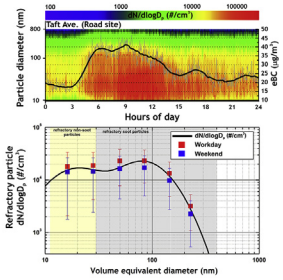

ARTICLE INFO

Article history:
Received 20 April 2017
Received in revised form
7 September 2017
Accepted 23 September 2017
Available online 27 September 2017

Keywords:
Refractory particle size distribution
Aerosol particle mixing state
Emission factors of refractory particles

ABSTRACT

Ultrafine soot particles (black carbon, BC) in urban environments are related to adverse respiratory and cardiovascular effects, increased cases of asthma and premature deaths. These problems are especially pronounced in developing megacities in South-East Asia, Latin America, and Africa, where unsustainable urbanization ant outdated environmental protection legislation resulted in severe degradation of urban air quality in terms of black carbon emission. Since ultrafine soot particles do often not lead to enhanced PM_{10} and $PM_{2.5}$ mass concentration, the risks related to ultrafine particle pollution may therefore be significantly underestimated compared to the contribution of secondary aerosol constituents. To increase the awareness of the potential toxicological relevant problems of ultrafine black carbon particles, we conducted a case study in Metro Manila, the capital of the Philippines.

Here, we present a part of the results from a detailed field campaign, called Manila Aerosol Characterization Experiment (MACE, 2015). Measurements took place from May to June 2015 with the focus on the state of mixing of aerosol particles. The results were alarming, showing the abundance of externally mixed refractory particles (soot proxy) at street site with a maximum daily number concentration of approximately 15000 #/cm^3. That is up to 10 times higher than in cities of Western countries. We also

* Corresponding author.
E-mail address: kecorius@tropos.de (S. Kecorius).

https://doi.org/10.1016/j.atmosenv.2017.09.037

found that the soot particle mass contributed from 55 to 75% of total street site $PM_{2.5}$. The retrieved refractory particle number size distribution appeared to be a superposition of 2 ultrafine modes at 20 and 80 nm with a corresponding contribution to the total refractory particle number of 45 and 55%, respectively. The particles in the 20 nm mode were most likely ash from metallic additives in lubricating oil, tiny carbonaceous particles and/or nucleated and oxidized organic polymers, while bigger ones (80 nm) were soot agglomerates. To the best of the authors' knowledge, no other studies reported such high number concentration of ultrafine refractory particles under ambient conditions. Inverse modeling of emission factors of refractory particle number size distributions revealed that diesel-fed public utility *Jeepneys*, commonly used for public transportation, are responsible for 94% of total roadside emitted refractory particle mass.

The observed results showed that the majority of urban pollution in Metro Manila is dominated by carbonaceous aerosol. This suggests that PM_{10} or $PM_{2.5}$ metrics do not fully describe possible health related effects in this kind of urban environments. Extremely high concentrations of ultrafine particles have been and will continue to induce adverse health related effects, because of their potential toxicity. We imply that in megacities, where the major fraction of particulates originates from the transport sector, PM_{10} or $PM_{2.5}$ mass concentration should be complemented by legislative measurements of equivalent black carbon mass concentration.

1. Introduction

In year 2050, two thirds of the World's population that is more than 6.5 billion people, will be living in towns and cities (Floater et al., 2014). Asia is predicted to accommodate over half of the planet's population in numerous megacities with more than 10 million inhabitants. Previous studies already highlighted the adverse health risks due to urbanization in New Delhi (India), Beijing (China), Dhaka (Bangladesh) and other cities (e.g. Gurjar et al., 2010 and references therein). As the megacities grow, ranking of the urban areas in terms of their population size, socio-economic, infrastructural and environment-related parameters become increasingly important. It is believed that these rankings could help to develop the mitigation strategies, which are expected to improve the sustainability of megacities worldwide (Gurjar et al., 2008). Environment-related parameters often included ambient concentrations of criteria pollutants, such as total suspended particulate matter (TSP), which became an important subject in air quality legislation that has been implemented globally in the past few decades. For example, the United States Environmental Protection Agency (US EPA) started to regulate the mass concentration of PM_{10} in 1988, and $PM_{2.5}$ in 1997 (particulate matter with aerodynamic diameter smaller than 10 μm and 2.5 μm, respectively) (Aggarwal et al., 2012). In European Union - New Air Quality Directive was enforced on 11 June 2008, which became strictest acts of legislation worldwide concerning PM_{10} emissions (Marco and Bo, 2013). To improve the living environment and to protect human health, the State Council of China has updated their old environmental legislation in 2012 including standards for never before controlled $PM_{2.5}$ values (Zhang and Cao, 2015).

While TSP, PM_{10} and $PM_{2.5}$ are the most commonly used metrics to address health effects (Pope and Dockery, 2006), there are several major reasons why particulate matter mass may need the complementary measurements in supporting the evidence of the air pollution-related health risks. Firstly, studies shown that exposure to high mass concentration of PM_{10} sea-salt does not result in any cardiovascular symptoms (Mills et al., 2008). This can be important when cities are located near sea/ocean coast where PM_{10} aerosol particle mass might be elevated due to high concentrations of airborne sea-salt. Secondly, re-suspended road dust was also shown to contribute to urban PM_{10} and $PM_{2.5}$ concentrations (Abu-Allaban et al., 2003). While the PM metrics would suit well to regulate air quality in situations where the re-suspended coarse mode particles are dominant, the contribution of ultrafine soot particles to health-related effects may be then overlooked. This is because, being less than 100 nm in diameter, the soot particles constitute only a minor fraction of PM mass. It means that even high soot particle number concentrations result in relatively low particulate matter mass concentrations. And yet, high number of these particles can deeply penetrate into the respiratory system increasing the risks of asthma, cancer, heart malformations, and even premature deaths (Ibald-Mulli et al., 2002; Strak et al., 2010). The importance of particle number and surface area in health-related issues was already highlighted by previous studies (Peters et al., 2004; Vinzents et al., 2005; Janssen et al., 2011; Brown et al., 2001). These studies suggest that the supplementary parameters, to evaluate air quality and possible health related risks, are of a great need. Especially in regions with unsustainable urbanization and growing traffic congestions, where controlled PM10 mass concentrations are reported to be within preset limits.

An exemplary case of unsustainable urbanization is the megacity of Metro Manila, the capital of the Philippines. It accounts for more than 12.9 million inhabitants and 2.3 million registered motor vehicles as of 2015 (information available at https://psa.gov.ph/content/population-national-capital-region-based-2015-census-population-0 and http://www.lto.gov.ph/transparency-seal/annual-reports/file/19-annual-report-2015.html (accessed March 4th, 2017)). Here, the inefficient public transport system and the rapid increase of vehicular fleet resulted in congested streets being filled with private cars, taxis, old buses and public utility *Jeepneys* (PUJs). Equipped with pre-EURO diesel engines, PUJs emit high concentration of combustion generated aerosol particles, which in turn became a dominant aerosol in the urban atmosphere. The emission inventories reported that traffic-related sources are responsible for more than 71% of the total country's particulate matter emission in the Philippines (Vergel and Tiglao, 2013). In the National Capital Region (NCR), the local Department of Environment and Natural Resources report that 90% of emissions can be attributed to mobile sources (information available at http://www.aecen.org/sites/default/files/country_report_the_philippines.pdf (accessed March 4th, 2017)).

To address the air pollution problem, ambient air quality guidelines were set by the Philippine Clean Air Act (CAA) on 23 June 1999 (CAA is available for download at http://emb.gov.ph/wp-content/uploads/2015/09/RA-8749.pdf (accessed March 9th, 2017)). This legislation covered limits for ambient levels of major air

pollutants, including PM_{10}. Short-term (24-hr) and long-term (annual) averages of PM_{10} of 150 and 60 μg/m^3, respectively, were set as National Ambient Air Quality Guideline Values (NAAQGV). Until recently, the $PM_{2.5}$ has been also included in NAAQGV, with short-term and long-term guidelines of 50 and 25 μg/m^3, respectively, as of January 2016. Since the CAA was declared, long-term measurements (during 2001–2008) of PM_{10} showed that annual PM_{10} is consistently below the NAAQGV (Zhu et al., 2012). In a study by Asian Institute of Technology, the Manila Observatory (MO) performed long-term PM_{10} and $PM_{2.5}$ measurements from 2001 to 2004 and reported that seasonal average PM_{10} concentrations in Metro Manila were almost within the World Health Organization (WHO) 24-h Air Quality Guideline (AQG) of 50 μg/m^3. Despite relatively low particulate matter mass values the incidences of lung cancer are rapidly increasing (Laudico et al., 2010). It suggests that the megacity of Metro Manila faces a much different pollution problem than previously reported cases in other, more industrial urban environments.

The main objective of this study was to characterize the physical properties of traffic-related carbonaceous particles in a busy street canyon in Metro Manila, Philippines. High-quality emissions data, including number size distributions of particles, is in great demand and is believed to facilitate the improvement of megacities' air quality (Gurjar et al., 2008). In this study, we used equivalent black carbon (eBC) mass concentration and refractory particle number size distributions (r-PNSD) (as a soot proxy) to illustrate that these parameters may be a valuable indicator to evaluate air quality and possible health related risks in urban environments. For the first time in this region, size segregated refractory particle emission factors (EFs) of light duty vehicles (LDVs) and PUJs were calculated. This study is also a continuation of our previous work where we found that the social behavior of the city dwellers in Metro Manila is significantly different than in Western and other Asian countries (Kecorius et al., 2017). It may subject the citizens of Metro Manila to higher personal exposure to carcinogenic species. This work has a potential to bridge the gap between the increasing incidence of lung cancer and the growing air pollution problem in the Philippines. Moreover, results from this study can be applied to other similar environments where the contribution of the transport sector to the worsening air quality and possible health effects on the city population needs to be assessed.

2. Experimental methods

The measurements were performed as part of an intensive aerosol research experiment called the "Manila Aerosol Characterization Experiment 2015" (MACE, 2015). MACE was carried out and jointly organized by the Leibniz Institute for Tropospheric Research (TROPOS) and the Consortium "Researchers for Clean Air" (RESCueAir) from March to June 2015. The RESCueAir consortium includes researchers and academics from the University of the Philippines (UP) Diliman, the Manila Observatory (MO), Ateneo de Manila University (ADMU), De La Salle University (DLSU), and the Philippine Nuclear Research Institute (PNRI).

2.1. Measurement site

The aerosol measurement container was situated at the roadside of Taft Avenue (14.56N, 120.99E) in the vicinity of De La Salle University, Manila, Philippines (Fig. 1), around 100 m to a traffic light. Taft Avenue is composed of six lanes, three of which are southbound. The measurement container was placed so that it occupied one of the lanes. One notable feature of the avenue was the suspended railway, which is approximately 7 m high. The aerosol container was air-conditioned to 24 °C to ensure the stability of aerosol instrumentation. PM_{10} inlet (16.67 l/min, 5 m a.s.l), followed by two 1.5 m Nafion dryers and an automatic drying chamber (Tuch et al., 2009) secured particle size cut-off at 10 μm and a constant relative humidity (RH) below 30%. Short and vertical conductive tubes were used inside the container to minimize particle losses in the sampling line. At Taft Avenue, continuous measurements were performed during the period of 16 May to 11 June 2015.

Driving conditions in the avenue can be described as follows. The lowest fleet count, regardless of the vehicle category, was observed during the early morning hours (03:00 to 04:00 a.m.) (see Fig. 2). During this time period vehicles were moving freely at speeds of approx. 30–50 km per hour. At this time, only a traffic light was the main reason for vehicles to brake, idle or accelerate. A rapid increase of fleet density was observed by around 05:00 to 07:00 a.m., which remained almost constant until 18:00 p.m.. The situation aggravated during three distinct rush hours (morning, lunch, and afternoon, Fig. 2), when vehicles were standing in one place "bumper-to-bumper" for about 5–10 min. In general, we can conclude that the sampled particulate pollution was resulting from braking, idling, and accelerating vehicles as well as free traffic flow (usually at night). We believe that such driving conditions are valid to represent the majority of cases of Metro Manila's traffic flow. An example of traffic flow at Taft Avenue can be found at https://youtu.be/5cT0xSBBasE.

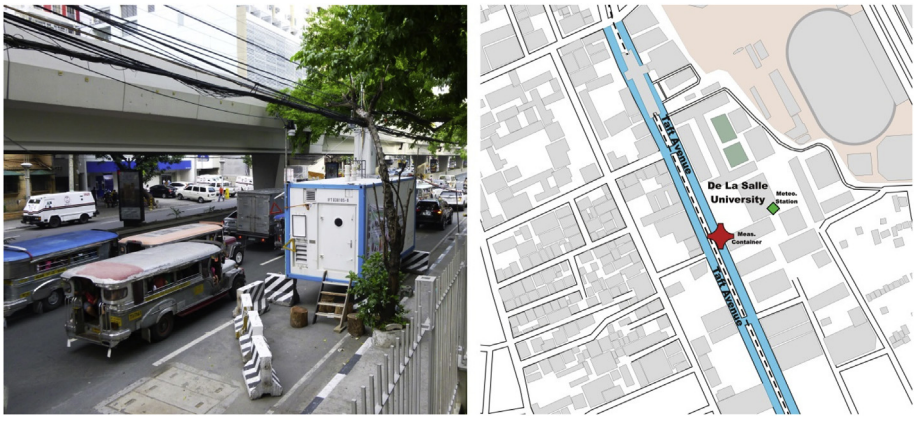

Fig. 1. A photo of the instrument container on Taft Avenue (left) and the sketch of the measurement site (right). Green diamond shows the location of rooftop meteorological station and the red mark – instrument container.

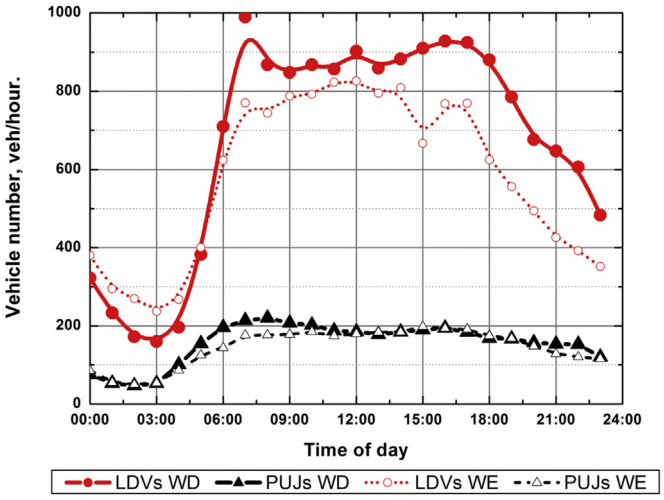

Fig. 2. The traffic intensity of light duty vehicles (LDVs) and public utility *Jeepneys* (PUJs) during working days (WD) and weekends (WE).

2.2. Instrumentation

2.2.1. Volatility Tandem Differential Mobility Analyzer (V-TDMA)

In this study size segregated mixing state of aerosol particles was determined using TROPOS-type V-TDMA system. Detailed instrument description can be found in Philippin et al. (2004) and will not be presented here. Briefly, dried quasi-monodisperse particles, selected by a Differential Mobility Analyzer (DMA-1, Hauke-type, 11 cm effective length, sheath flow rate 5 l/min) is split into two flows, which are then directed to a Condensation Particle Counter (CPC-1, TSI model 3010) and a thermal conditioning unit (TD). In the TD, the aerosol particle flow is automatically alternated between two temperatures of 25 and 300 °C. Lower temperature scans were used to calibrate the kernel function in a data inversion routine presented by Gysel et al. (2009). The volatility distributions were measured by a second DMA in conjunction with a CPC-2 (both identical to the DMA-1 and CPC-1). The total sample flow rate of the system was 1 l/min (defined by two CPC flows of 0.5 l/min). The residence time inside the heating column was 0.3 s, which was shown to be enough to evaporate sulfate, nitrate and volatile and semi-volatile organic material shells from black carbon cores (Burtscher et al., 2001; Philippin et al., 2004). We chose six diameters to be selected by DMA-1: 20, 35, 63, 110, 200 and 350 nm. Please note that these are mobility and not volume-equivalent diameters. The methodology used to calculate a volume-equivalent diameter (later used in the text) is described in paragraph 2.3.1. The full scan cycle took less than 1 h.

2.2.2. Mobility Particle Size Spectrometer (MPSS)

Dry (RH<30%) particle number size distributions (PNSD), in a mobility size range from 10 to 800 nm, were measured with a TROPOS-type MPSS (Wiedensohler et al., 2012). The system uses a Hauke-type DMA (effective length of 28 cm) together with a CPC (model 3772, TSI Inc., USA, flow rate 1 l/min). The time resolution of up-and-down scan was 5 min. However, we decoupled up-and-down scans to increase the time resolution to 2.5 min. Electrical particle mobility distributions were inverted to PNSDs using the inversion algorithm presented by Pfeifer et al. (2014). The final PNSDs were corrected for transmission losses in the sampling lines using the method of equivalent length and CPC counting efficiencies (Wiedensohler et al., 1997). Sizing accuracy in MPSS and V-TDMA systems were controlled using nebulized polystyrene latex spheres (PSL, Thermo Scientific™, Duke Standards™) of 203 nm. High voltage supply offset calibration, instrument flows and tests for leakage were performed on a regular basis (once per week).

2.2.3. Supplementary measurements

To check the validity of retrieved refractory particle number size distributions as a proxy for soot, we also used a Multi-Angle Absorption Photometers (MAAP Model 5012, Thermo, Inc., Waltham, MA USA; Petzold and Schönlinner, 2004) to measure equivalent black carbon (eBC) mass concentration. The instrument accounts for multiple scattering effects and absorption enhancement due to reflections from the filter. The operating wavelength of 637 nm is chosen to minimize the interference with organic material and mineral dust (Sun et al., 2007; Müller et al., 2009). To save the filter medium in the heavily polluted environment, the MAAP flow was adjusted to 3 l/min using a custom made nozzle. The temporal resolution of the instruments was set to 1 min.

To be able to model the emission factors (EFs), the vehicles were counted manually from continuously recorded street site videos (an example video is available at https://youtu.be/5cT0xSBBasE). The counts were performed for the whole measurement period and all sequential hours of the day and are presented in Fig. 2. The vehicular fleet was divided into 2 categories of light duty vehicles (LDVs) and public utility Jeepneys (PUJs), each contributing 80% and 20% to the total fleet, respectively. The meteorological parameters, such as wind speed/direction, temperature and relative humidity were measured by the meteorological station at the rooftop of De La Salle University.

2.2.4. Meteorological conditions

The MACE 2015 measurement campaign took place during two seasons – dry and wet. According to Akasaka (2010) and Villafuerte et al. (2014), the dry season lasts from December to May, with the rest of the year being affected by Southwest monsoons and tropical cyclones. Despite this general classification, we did not experience any prolonged rainfall, which may have influenced the quality of our measurements. Short rains occurred on some occasions, and although it did not affect the measurement results, we have eliminated data from those periods in our succeeding analyses.

The daily average of temperature, wind speed and RH during the measurement period was 31 ± 2 °C, 0.9 ± 0.6 m/s and 69 ± 8%, respectively. The maximum temperature and wind speed was recorded in midday reaching 33 ± 1 °C and 1.7 ± 0.9 m/s. After 1.00 p.m., the values begin to drop gradually and reached the minimum of 29 ± 1 °C and 0.5 ± 0.3 m/s at 5.00–6.00 a.m. local time (LT). Maximum (77 ± 4%) and minimum (60 ± 4%) RH values were measured at 5.00 a.m. and midday, respectively ("±" shows standard deviation).

2.3. Data processing

In the next sections, we will briefly explain the procedures used to evaluate measurement data. A more detailed description about the data processing can be found in the supplementary material (SP-1).

2.3.1. Retrieval of refractory particle number size distribution (r-PNSD)

To retrieve r-PNSD we used the data from the MPSS and V-TDMA systems (Wehner et al., 2004). For the non-spherical particle consideration, we have recalculated the particle mobility diameters (d_m) to volume-equivalent diameters (d_{ve}) using the formalism presented by Pfeifer et al. (2014) and Park et al. (2004). This includes the division of d_m by size-dependent aerodynamic shape factor ($\chi(d_{ve})$) as follows:

$$\frac{d_m}{C_C(d_m)} = \chi(d_{ve})\frac{d_{ve}}{C_C(d_{ve})}, \quad (1)$$

where C_C is the Cunningham correction. Using the results from Park et al. (2004) we defined the empirical, size-dependent $\chi(d_{ve})$ as:

$$1.9 - \frac{0.8}{1+\exp\left(\frac{d_m-320}{190}\right)}. \quad (2)$$

TDMA inversion routine (Gysel et al., 2009) was used to invert volume-equivalent raw V-TDMA scans to Shrink Factor – Probability Density Function (SF-PDF). After analyzing all measured volatility distributions, the refractory particle SF-PDFs were divided into two groups: SF<0.9 and SF>0.9 to determine more-volatile (MV) and less-volatile (LV) particles (Fig. 3). The integration of SF-PDF from SF = 0.9 to SF = 1.1 gave us the number fraction of LV particles, $f_{N,LV}$. The r-PNSD can be then reconstructed by multiplying measured PNSD with $f_{N,LV}$ in a measured PNSD size range. The retrieved r-PNSDs were then fitted with log-normal distributions.

2.3.2. Estimation of emission factors (EFs)

Size-segregated EFs of refractory particles were estimated utilizing Operational Street Pollution Model (OSPM, Berkowicz, 2000). The model's applicability was proven by numerous worldwide studies in the past decade (e.g. Kakosimos et al., 2010). The references to detailed physical principles of the model are provided in Kakosimos et al. (2010). Shortly, the concentration of pollutants in the street canyon depends on both emission and dilution. The general purpose of OSPM is to predict the concentration of pollutants by combining the plume and box models. To run the model, the input of accurate street canyon geometrical configuration (building locations, heights, street orientation against north), rooftop meteorological conditions (wind direction and wind speed), and the emission factors of corresponding pollutants are required. However, in our case, the desired parameter to be estimated is the EFs, while the measured one is particulate pollutant concentration. This is known as inverse modeling approach, widely applied in previous studies to determine the EFs based on in-situ measurements (e.g. Palmgren et al., 1999; Rose et al., 2006; Brizio et al., 2007). The emission factor, q_k, for the kth vehicle category can be determined as:

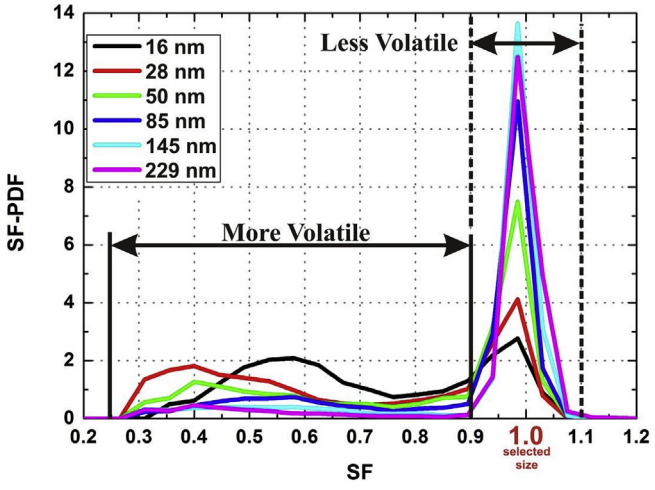

Fig. 3. Averaged Shrink Factor-Probability Density Function (SF-PDF) of size segregated refractory particles.

$$q_k\left[\frac{1}{km\cdot veh}\right] = \left(\frac{\Delta C}{F}\right) \Big/ \sum_k N_k\left[\frac{veh}{s}\right], \quad (3)$$

where F is the dilution function calculated using OSPM, which mainly depend on meteorological parameters and street geometry, N_k is the traffic flow of k^{th} vehicle category and ΔC is the pollutant concentration increase due to the traffic in a street canyon. The average, or in other words, total fleet emission factor can then be found by solving the simple linear regression:

$$\Delta C = q\cdot(F\cdot N_{veh}). \quad (4)$$

Because the total emission along the street is a superposition of separate vehicle group emissions, we can split the emission of the fleet into the emission of separate vehicle groups. If we assume that the total vehicle fleet can be approximated by LDVs and PUJs, we can rewrite equation (4) as:

$$\Delta C = q_{LDVs}\cdot F\cdot N_{LDVs} + q_{PUJs}\cdot F\cdot N_{PUJs}, \quad (5)$$

where q_{LDVs}, N_{LDVs}, q_{PUJs}, N_{PUJs} are the emission factors and vehicle numbers for the LDVs and PUJs vehicle groups, respectively. Equation (5) can then be solved by bivariate linear regression resulting in a plane, in which the slopes represent EFs of different vehicle fleets. The results of the bivariate linear regression can be found in the supplementary material (SP-2).

The concentration of pollutants in the street canyon is the superposition of the (1) urban background, which is the result of both regional pollution and the contributions from the city itself, and the (2) direct tailpipe emissions from the bypassing traffic. Several ways to estimate ΔC were presented in the literature (Kakosimos et al., 2010). It can be calculated using the background concentrations obtained from a nearby measurement station, which is not affected by direct emissions. Urban background and regional pollution models can also be used to calculate the concentration of background pollutants. Brizio et al. (2007) used averaged night-time street level concentrations as a representation for background pollution. However, we find these methods to be limiting as the nearby background measurements may not be available, the regional models may be time consuming and a night-time pollutant concentration does not necessarily represent the daytime background concentration variation. Therefore, we have used instead a new method to determine the background pollution concentrations at a street site. The direct vehicular emission can be easily spotted in MPSS as a sudden high-value particle number concentration increase followed by a consequent steep drop when the vehicles were passing the measurement container. According to Kakosimos et al. (2010, Fig. 5), these high values are the traffic fingerprints, while the values before and after this increase should represent urban background conditions. Following this logic, we have calculated the rolling minimum concentrations with a variable time window over all measurement period. As the rolling minimum window increased, the minimum values were found to get lower and vice versa. The compromise was made to use 1 h duration for a rolling minimum calculation by a trial and error approach. The results were comparable to a time variation of background factor in a positive matrix factorization (not shown here). This method proved to give a reasonable and smooth diurnal pattern of urban background pollutant concentration. An example case of the application of the proposed method is demonstrated in the supplementary material (SP-3).

3. Results and discussion

In this section we present and discuss the measurement results in the following order: first, in paragraph 3.1 the state of mixing of aerosol particles in terms of volatility; in paragraph 3.2 we present the derived refractory particle number size distributions; and last, the size-segregated emission factors of refractory particles are discussed in paragraph 3.3.

3.1. The state of mixing of aerosol particles

The daily variation of size-segregated Shrink Factor-Probability Density Function (SF-PDF) is shown in Fig. 4. A clear separation of a SF-PDF mode at SF~1 can be seen for particles with volume equivalent diameters greater than 50 nm. This mode gets increasingly dominant with increasing particle size, while smaller particles do not show such clear separation of SF-PDF. Moreover, a rather evident two mode pattern appears in SF-PDF for particles smaller than 50 nm. In this case, the transition region at 50 nm separates two groups of particles: smaller with bimodal volatility properties, and bigger, where particles become more uniform in their thermal properties. Interestingly, in experiments by Rader and McMurry (1986) the boundary between the nucleation and accumulation modes was found at 30 nm. Smaller particles were found to be more volatile than larger ones.

However, this type of volatility representation as shown in Fig. 4 is rather qualitative. More useful way to discuss particle thermal properties is to use integrated number fraction of less volatile particles ($f_{N,LV}$) and volume fraction remaining (VFR). The method to retrieve $f_{N,LV}$ is presented in section 2.3, while the VFR was directly extracted from TDMAinv routine "RetrVFRavg" wave (Gysel et al., 2009). The results of $f_{N,LV}$ and VFR are summarized in Table 1 and visually presented in Fig. 5 (as median, mean and the 5, 25, 75, 95-th percentiles). It can be seen that the major number fraction of less-volatile particles resides in a size range from 85 to 229 nm. Similar results were also observed in previous studies with a focus on pollution in urban environment (Wehner et al., 2004; Rose et al., 2006). In this study, the $f_{N,LV}$ and VFR increased up to 90% with increasing particle diameter. On the other hand, these values became as low as 30-50% for particles smaller than 50 nm. As it was already noted before, 50 nm seem to be the transition region between the Aitken and accumulation mode particles with slightly higher variability in particle volatility as represented by higher standard deviation (error bars in Fig. 5). This higher variability is mainly due to daily variation in $f_{N,LV}$ and VFR (not shown here). The $f_{N,LV}$ of 50 nm particle increased to its maximum value of approximately 70% at 8.00 a.m. and 4.00 p.m. At noon these values decreased to as low as 30%. All other size particles, except 50 nm, did not show such behavior and were rather uniform in their $f_{N,LV}$ and VFR values during the hours of day. This suggest that particles in 50 nm size range is most likely a mixture of directly emitted and particles from secondary aerosol production with higher volatility that were transported to the measurement site from the surrounding urban environments. The possible sources and processes

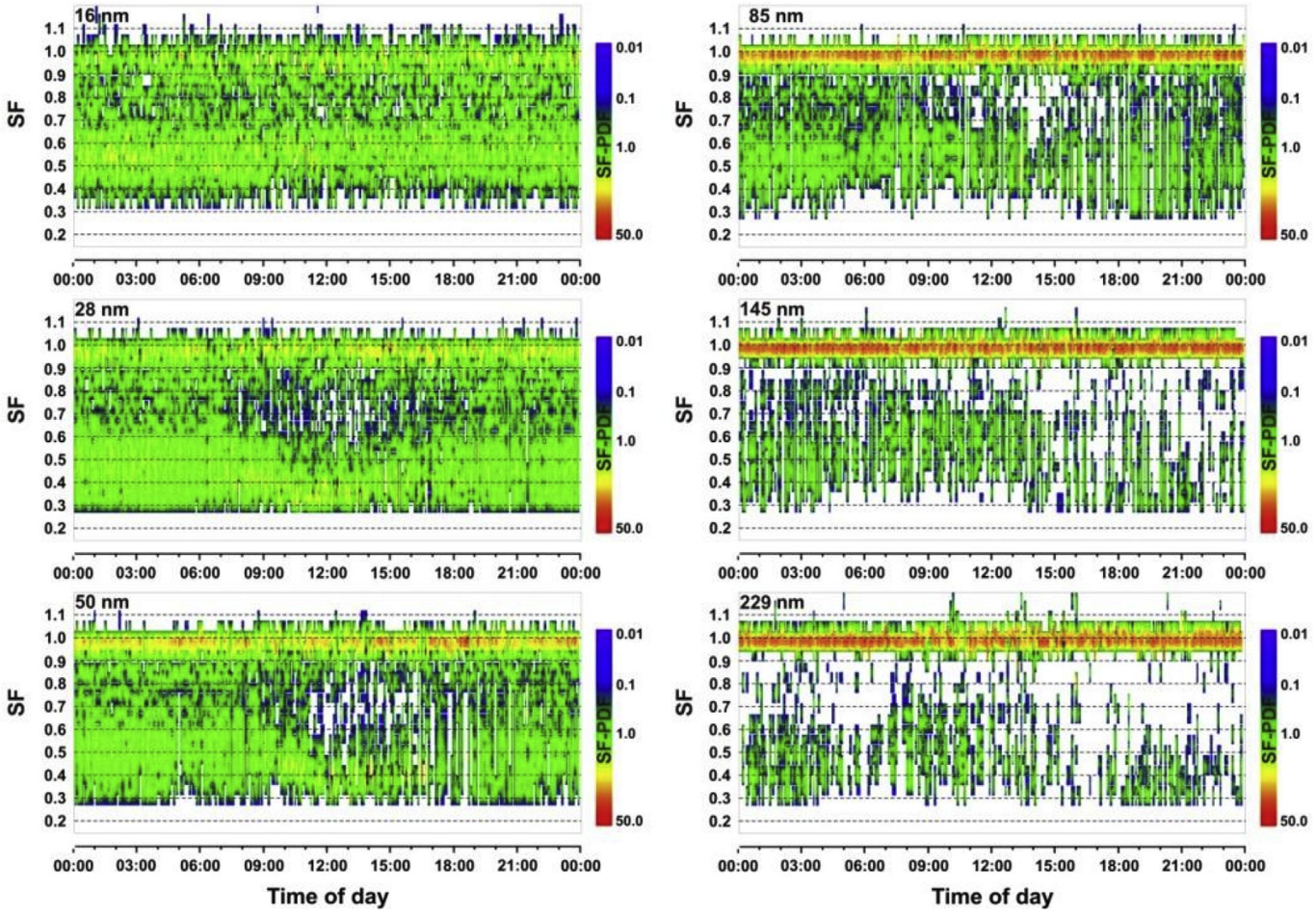

Fig. 4. The daily variation of size segregated particle Shrink-Factor Probability Density Function (SF-PDF).

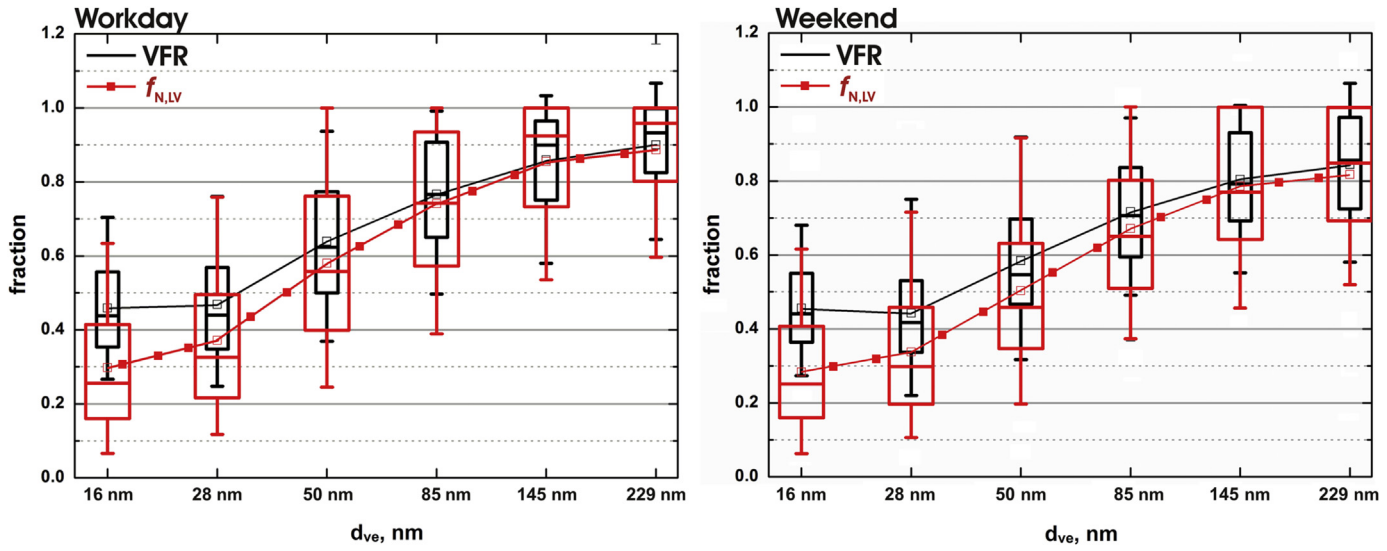

Fig. 5. The number fraction of less volatile ($f_{N,LV}$) and the volume fraction remaining (VFR) of refractory aerosol particles presented as 25th and 75th (box range), 5th and 95th (whiskers) percentiles, median (inner square) and mean (horizontal line inside the box).

Table 1
The average size segregated number fraction of less volatile ($f_{N,LV}$) and the volume fraction remaining (VFR) of refractory aerosol particles.

d_{ve}	16 nm	28 nm	50 nm	85 nm	145 nm	229 nm
$f_{N,LV}$						
Workday	0.30 ± 0.18	0.37 ± 0.20	0.58 ± 0.23	0.74 ± 0.20	0.86 ± 0.16	0.89 ± 0.14
Weekend	0.28 ± 0.17	0.34 ± 0.20	0.50 ± 0.22	0.67 ± 0.20	0.78 ± 0.18	0.82 ± 0.18
VFR						
Workday	0.46 ± 0.14	0.47 ± 0.16	0.64 ± 0.18	0.77 ± 0.16	0.86 ± 0.14	0.90 ± 0.13
Weekend	0.46 ± 0.13	0.44 ± 0.16	0.58 ± 0.18	0.71 ± 0.16	0.80 ± 0.15	0.84 ± 0.16

determining the observed particle mixing state will be discussed later in this paragraph.

Another interesting feature characterizing the state of mixing of aerosol particles can be seen from a difference between VFR and $f_{N,LV}$ (Fig. 5). We note that for the $f_{N,LV}$ calculation, we have used only a certain SF range (more details in paragraph 2.3.1.), while the VFR represents the full size range volatility spectrum. For this matter, VFR $\geq f_{N,LV}$ is always true. From Table 1 one can see that in the size range from 85 to 229 nm particle, $f_{N,LV}$ and VFR agree within 3% (*p-value* > 0.05, see supplementary material SP-4). This result suggests that the VFR in this size range can be almost entirely explained by $f_{N,LV}$. In other words, more than 97% of VFR in this size range are externally mixed refractory particles with no/or minimal volatile coating. The difference between $f_{N,LV}$ and VFR starts to increase with decreasing particle size. In a size range from 16 to 50 nm, $f_{N,LV}$ and VFR on average agree within 20% (*p-value*<0.05). This result suggests that as the particle diameter increased, aerosol particles had almost no volatile coating. While smaller particles seemed to disobey this rule and became more volatile with decreasing particle size.

Comparing working days (WD) versus weekends (WE), we found that VFR and $f_{N,LV}$ are from 6 to 9% lower on WE than WD (for particles more than 28 nm, *p-value*<0.05). Moreover, the difference between VFR and $f_{N,LV}$ is more profound on WE than WD (Fig. 5). One possible explanation for this could be lower traffic intensity on weekends (see Fig. 2). Although the number of heavy duty vehicles during WE did not change significantly compared to WD, the total number of vehicles was found to be somewhat lower. As a result, lower concentrations of pollutants were emitted to the urban environment. This allows higher fraction of volatile material to condense onto a single particle surface during particle ripening process compared to the conditions when higher number of particles would be present. At this stage it is important to discuss which processes and particles might be contributing to our observed thermal particle properties.

In this study, we used the V-TDMA system with a thermal conditioning unit set to 300 °C. Previous studies showed that there is a large variety of species that may remain refractory when heated to 300 °C. For example, inorganic salts were shown to decompose between 400 and 1700 °C, (Knudsen et al., 2004). Low-volatility oxygenated organic aerosol may also contribute to the refractory fraction of atmospheric aerosol particles (Poulain et al., 2014). On the other hand, in polluted urban environments with predominantly diesel emissions, the refractory species that do not decompose at a temperature of 300 °C were attributed to soot particles (e.g. Rose et al., 2006; Ning et al., 2013; Kittelson and Kraft, 2014). These ultrafine particles were found to form a mode with a geometric mean diameter of 80 nm. Non-exhaust-related particles, including re-suspended road dust, particles from mechanical wear of brake pads, tires, etc. may also contribute to measured refractory fractions. However, we do not expect these particles to influence our results because they mostly reside in a super-micrometer size range (Thorpe and Harrison, 2008). The findings from previous studies to some extent agreed with our measured $f_{N,LV}$ and VFR. The main difference was that we were also able to observe non-volatile particles in nucleation mode (in a range of 10–20 nm). While the observed refractory species at 80 nm mode are proven to be soot particles and its derivatives, including metal compounds from lubricating oil and engine wear, the origin of the smallest refractory particles (10–20 nm), observed in our study, is still not clear. Based

on previous studies, we speculate that these particles most likely were the non-volatile and semi-volatile lubricating oil compounds, organic polymers, ash from metallic additives, tiny carbonaceous spheres with different morphology than diesel particulates, as well as newly formed particles from species containing SO_3, gaseous sulfuric acid, heavy organics and other compounds that are released after thermal changes from the exhaust systems' surface (Engler et al., 2007; Tiitta et al., 2010; Karjalainen et al., 2014). This would explain our observed less volatile fraction of nucleation mode particles. The more volatile fraction of smallest particles may have been the result of incomplete volatilization of organic compounds (heavy hydrocarbons) due to residence time and/or temperature in the V-TDMA system and/or internally mixed sulfuric acid with non-volatile cores. Moreover, coagulation products between newly nucleated sulfur particles and refractory ashes may also contribute to more volatile particle number and volume fractions.

Prior to discussing the refractory particle physical properties, it is important to clarify how we use the term soot in this work. As it was already mentioned in previous studies, the refractory particles, which predominantly come from diesel vehicles, can be referred to as soot. However, in our case this is only partly equitable, mainly because of the presence of the smallest (10–20 nm) refractory particles. Bearing this in mind, we would like to introduce two terms used to distinguish between two different particle populations, derived from V-TDMA measurements. Further in the text, the refractory particles with a diameter >30 nm will be assigned to soot agglomerates, while the particles that are smaller than 30 nm will be cited as refractory particles. A particle number size distribution, in a range of 10–1000 nm, retrieved from the measurements of V-TDMA and MPSS will be specified as refractory particle number size distribution (r-PNSD). We believe that such a disclosure will lead to a better distinction between different particle populations. As it will be demonstrated later in section 3.4.2, our derived r-PNSD can be used as a proxy for soot particle number size distribution.

3.2. $PM_{2.5}$, number concentration and size distribution of refractory particles

In a previous section we presented the results of aerosol particle volatility measurements. Here we will focus on the refractory particle number size distribution (r-PNSD) and the importance of such measurements. As stated before, the Philippine ambient air quality guidelines set by the Clean Air Act, in terms of particulate matter, control only the levels of PM_{10}. This criteria pollutant was shown to be below national guidelines and almost within the World Health Organization (WHO) 24-h limit (Zhu et al., 2012). There might be several reasons for relatively low PM_{10} mass concentration in Metro Manila when compared to other megacities. For example, the Philippine Archipelago is unlikely to be affected by dust and sandstorms from remotely located deserts. Coastal location (enhanced dispersion), warm climate (no seasonal heating), low secondary aerosol production and high annual precipitation (particulate removal) may also substantially lower ambient PM_{10} concentrations (Oanh et al., 2006).

On the other hand, $PM_{2.5}$ concentrations that are measured since 2001, but not regulated until 2013, were reported to regularly exceed WHO limits (Zhu et al., 2012). This was also confirmed by our measurements (Fig. 6). $PM_{2.5}$ mass concentration determined by gravimetric method showed that $PM_{2.5}$ concentration was on average ~1.7 times higher than recommended WHO value. From $PM_{2.5}$ measurements and assuming that eBC (measured by MAAP as soot proxy) mainly reside in $PM_{2.5}$ size range we estimated that soot particles mass contributed from 55 to 75% of total $PM_{2.5}$. Moreover, on some occasion daily soot mass concentration was also much higher than the WHO recommended $PM_{2.5}$ value (e.g. 3rd of June, Fig. 6). It suggested that extremely high number concentrations of particles had to be emitted into the urban atmosphere in the form of soot in order to account for its contribution to $PM_{2.5}$ mass. Bearing this in mind and the fact that particle deposition in the respiratory system is size selective (Heyder et al., 1986), it is useful to determine refractory particle (as a proxy for soot) number size distribution to assess personal exposure to hazardous particulates.

Size-segregated number concentration of refractory particles can be calculated combining measurements of $f_{N,LV}$ together with ambient PNSD (see section 2.3.1). Because number fractions of refractory species were measured only for 6 preselected diameters, a continuous PNSD was retrieved using a log-normal fit. Refractory particle number concentration in the 10 - 1000 nm size range was then calculated from PNSD. Keeping in mind the terminologies we provided in the last paragraph of section 3.1, the results of refractory particle physical properties are shown in Fig. 7, Fig. 8 and Table 2. Since the difference between workdays and weekends was negligible, we excluded this information from the discussion for redundancy.

In Fig. 7 it can be seen that the refractory particle (rp) number concentration (black solid line) start to increase from its minimum value of $6 \cdot 10^3$ rp/cm^3 at around 3.00 a.m. The concentration of particles doubled by 5.00 a.m. reaching $1.5 \cdot 10^4$ rp/cm^3. These high values were sustained until around 2.00 p.m. when it started to decline to $1 \cdot 10^4$ rp/cm^3 at around 3.00–8.00 p.m. For a comparison, average soot (refractory particles in a 80 nm mode) number concentration was reported to be between $4 \cdot 10^3$ and $6 \cdot 10^3$ rp/cm^3 in a street canyon in Germany (Rose et al., 2006). Our observed steep increase in the refractory particle number concentration is most likely a result of increased traffic intensity (Fig. 2). Diesel powered PUJs and LDVs filled the streets at around 3.00 a.m. By 6.00–7.00 a.m. the number of vehicles was already at its maximum, which when coupled with low wind speeds and stable atmospheric conditions (weak convection mixing due to solar radiation minimum) resulted in the accumulation of pollutants in the street canyon. A slight increase in vehicle flow intensity can also be observed during rush hours (6.00–9.00 a.m., noon, and 4.00–5.00 p.m.). During the daytime (6.00 a.m.–6.00 p.m.), the number of vehicles on the street remained rather stable. The intensity of traffic density declined from 6.00 p.m. to its minimum at 3.00 a.m.

The decrease in refractory particle number concentration started at around 2.00 p.m., which is approximately 4 h before the decline of the traffic intensity. This observation suggests that not only traffic intensity, but also other factors affected diurnal variation of refractory particle number concentration. To address this question, we investigated the relationship between number of particles and the wind speed and direction (see supplementary material SP-5). As expected, the lowest number concentrations of particles were observed when the prevailing winds were from the Southwest, West and Northwest sectors, which are opposite to the roadside. When the winds were coming from the Southeast, East and Northeast sectors (direction of the road), particle number concentrations were determined to be at least two times higher. Diurnal variation in wind speed and direction showed that the lowest wind speed (approx. 0.4 m/s) was observed between midnight and 6.00 a.m. (see supplementary material SP-6). By 8.00 a.m. it gradually built up reaching maximum values of approx. 2 m/s between midday and 5.00 p.m. The strongest winds were consistently prevailing from directions opposite to the roadside (with respect to the measurement container). This specific diurnal variation of the wind speed and direction has created conditions in which the less polluted air from the urban background diluted the

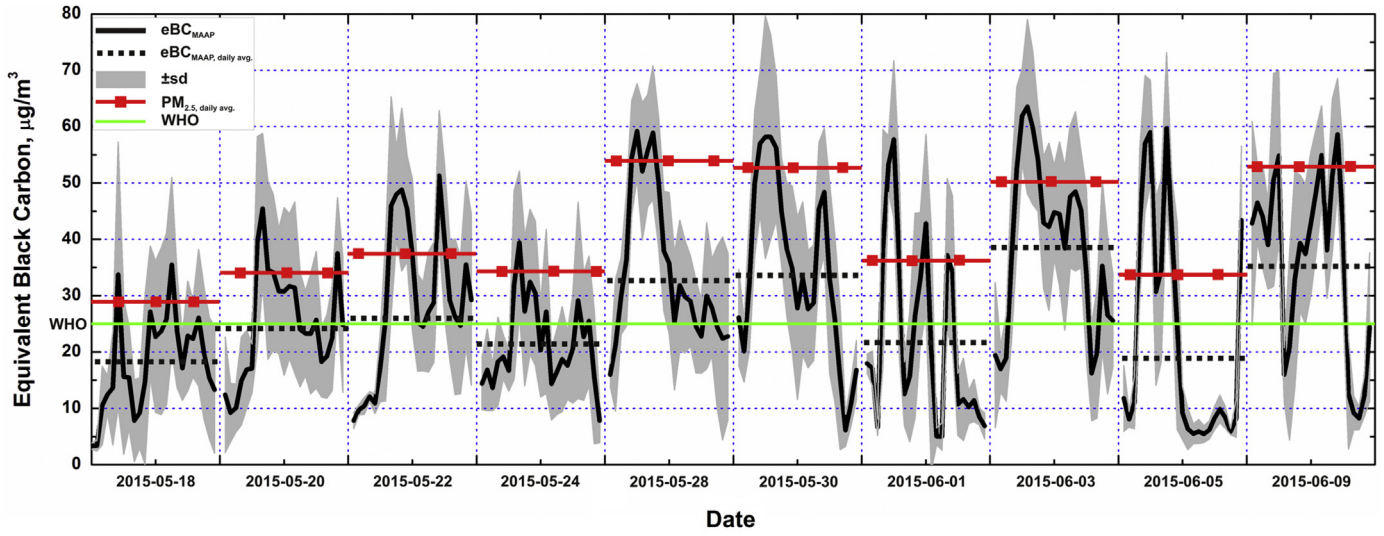

Fig. 6. Equivalent black carbon (eBC, as proxy for soot) mass concentration measured with MAAP, gravimetric $PM_{2.5}$ mass concentration derived from 24-h filter samples and World Health Organization (WHO) guideline value for 24-h average mass concentration of $PM_{2.5}$. Grey shaded area shows variability (standard deviation) over sampled period of time.

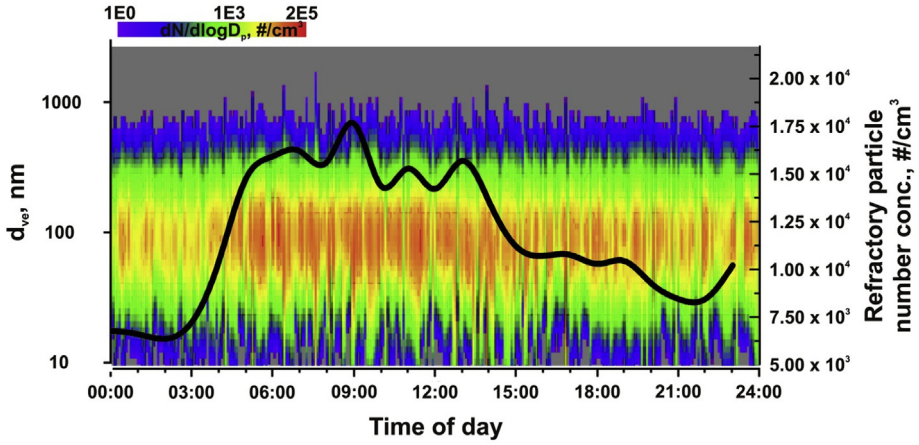

Fig. 7. Refractory particle (soot proxy) number size distribution (contour plot) and the integrated number concentration (black line).

street canyon aerosol resulting in observed soot particle number concentration decrease. The dilution, however, did not change r-PNSD shape, only its strength (Fig. 7). This is most likely because the transported background aerosol is a result of the same type of emissions from the surrounding streets.

The averaged r-PNSD and corresponding surface area and volume size distributions are presented in Fig. 8. It can be seen that r-PNSD is a superposition of two particle modes: refractory non-soot and refractory soot, with the geometric mean diameters of 20 and 80 nm, respectively. Corresponding mode contribution to total refractory particle number was 45 and 55%, respectively. When compared with previous studies, the distinct difference was found in smaller particle mode. For example, using the same methodology, Rose et al. (2006) derived r-PNSD comprising of only bigger mode particles. The same was observed in a study by Ning et al. (2013), who reported that eBC aerosols from diesel vehicles contained mostly unimodal particles at around 80–100 nm in measured particle number size distributions. We observed that with daytime the number concentration of particles bigger than 50 nm increased all together, while the number concentration of <50 nm particles displayed a slightly different pattern (see supplementary material SP-7). These smallest particles formed a unique concentration maximum just around noon, when solar radiation was at its strongest, while a bigger size particle concentration closely followed the trend of vehicle flow intensity. This further suggested that the smallest observed refractory particles might be the result of nucleated low volatility organics, or a subsequent condensation of semi-volatile organics onto nucleated sulfate particles and their later oxidation causing the formation of non-volatile organic polymers.

We find the presence of the smallest refractory particles to be very intriguing not only because they appear to be a signature of a highly polluted urban environment where old technology engines are still in use, but also because of their abundance. Despite their negligible contribution to overall particulate mass, these very fine particles may penetrate deep into the respiratory system. Moreover, because polycyclic aromatic hydrocarbon molecules were found to be a key precursor in carbonaceous particle formation, these smallest particles may play a significant role in health related effects (Kittelson and Kraft, 2014; Abdel-Shafy and Mansour, 2016).

3.3. Size-segregated emission factors of refractory particles

The derived refractory particle number size distributions from

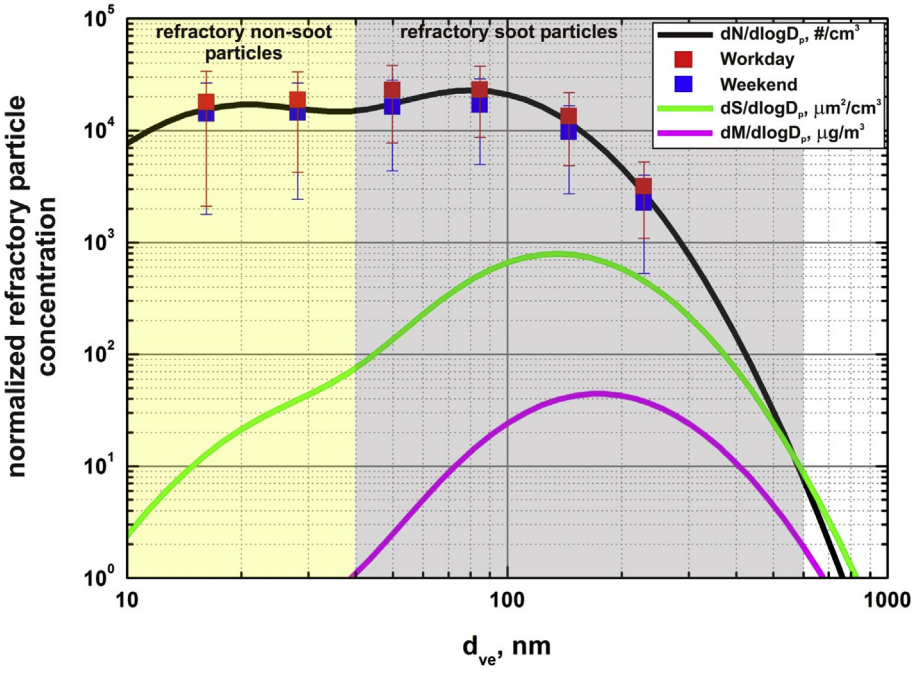

Fig. 8. Average refractory (yellow shade) and soot (grey shade) particle number, surface area and mass size distributions. Solid lines show distributions after a log-normal fit. Error bars indicate the standard deviation. For example, refractory particle number size distribution is shown by a black solid line with y-axis as dN/dlogD$_p$, #/cm^3.

Table 2
Campaign average of size segregated and normalized refractory particle number (dN/dlogD$_p$, #·10^4/cm^3), surface (dS/dlogD$_p$, μm^2/cm^3) area and mass (dM/dlogD$_p$, μg/m^3) concentrations. Variability (standard deviation) is presented after "±" sign.

d$_{ve}$	16 nm	28 nm	50 nm	85 nm	145 nm	229 nm
Workday						
Number conc.	1.79 ± 1.58	1.88 ± 1.46	2.30 ± 1.53	2.31 ± 1.44	1.34 ± 0.85	0.32 ± 0.21
Surface conc.	15 ± 13	47 ± 36	180 ± 120	520 ± 325	890 ± 560	520 ± 342
Mass conc.	0.1 ± 0.08	0.5 ± 0.4	3.3 ± 2.2	16.1 ± 10	46.9 ± 29.8	43.4 ± 28.5
Weekend						
Number conc.	1.42 ± 1.24	1.45 ± 1.20	1.63 ± 1.19	1.70 ± 1.20	0.97 ± 0.70	0.23 ± 0.17
Surface conc.	12 ± 10	36 ± 30	127 ± 93	383 ± 271	644 ± 464	372 ± 285
Mass con.	0.07 ± 0.06	0.4 ± 0.3	2.3 ± 1.7	11.8 ± 8.4	34.2 ± 24.6	31.1 ± 23.8

VTDMA - MPSS measurements and meteorological data together with vehicle fleet count allowed us to determine size-segregated refractory particle number, surface area and mass emission factors (EFs). Moreover, apart from calculating the average EFs of refractory particles, we were also able to distinguish EFs between different fleets, LDVs and PUJs. The detailed methodology for determining EFs can be found in section 2.3.2. Information about EFs is important not only for urban air quality modeling, but it also helps to understand, which type of vehicles contribute most to observed particle physical-chemical properties. The results of derived size-segregated EFs are presented in Fig. 9 and summarized in Tables 3 and 4. We found average vehicle refractory particle number and mass EFs to be 3.29·10^{14} rp/(km·veh) and 0.313 g/(km·veh), respectively. Separation between different fleets gave corresponding refractory particle number EFs values of 9.79·10^{13} and 1.15·10^{15} rp/(km·veh) and refractory particle mass EFs of 0.027 and 1.618 g/(km·veh) for LDVs and PUJs, respectively. From here, it can be seen that PUJs emit 11.7 times more particle in terms of number and 61.3 times more particles in terms of mass when compared to LDVs. Comparing these values to the European Union (EU) emission standards (Table 3), it is clear that the particle number emission from PUJs in Metro Manila exceeds Euro 6 target value of 6.0·10^{11} particles/(km·veh) (6.0·10^{12} particles/(km·veh) within the first three years from Euro 6 effective dates) by up to 2000 times. We have to note that this difference may be even higher if total, and not only refractory particle number was considered. Until 2014, EU emission regulation did not include particle number as one of the standards, instead, particulate matter mass (PM) was used. In terms of PM, LDVs refractory particle mass EFs in Metro Manila falls in the range of EURO 4 emission regulation. While PUJs, with an approximate weight of 3500 kg (Braganza et al., 2007) and being in the category of light commercial vehicles in EU EURO standards, showed 6.6 times higher PM emission even when compared to the outdated standard from 1992 (EURO 1).

Furthermore, from Fig. 9, it can be seen that LDVs and PUJs emit not only different number concentrations but also considerably different sizes of particles. Starting with LDVs, in this vehicle fleet most of refractory particles in terms of their number concentration were emitted in a size range from 10 to 200 nm. These findings were consistent with laboratory studies as well as "car chasing" experiments, which reported that not only diesel, but also gasoline driven vehicles emit refractory particles with geometric mean diameter shifted towards smaller particle sizes when compared to diesel emissions (Karjalainen et al., 2014). The larger diameter particles (approx. 200 nm) in this study were most likely soot aggregates emitted by LDVs. The emission of these bigger particles

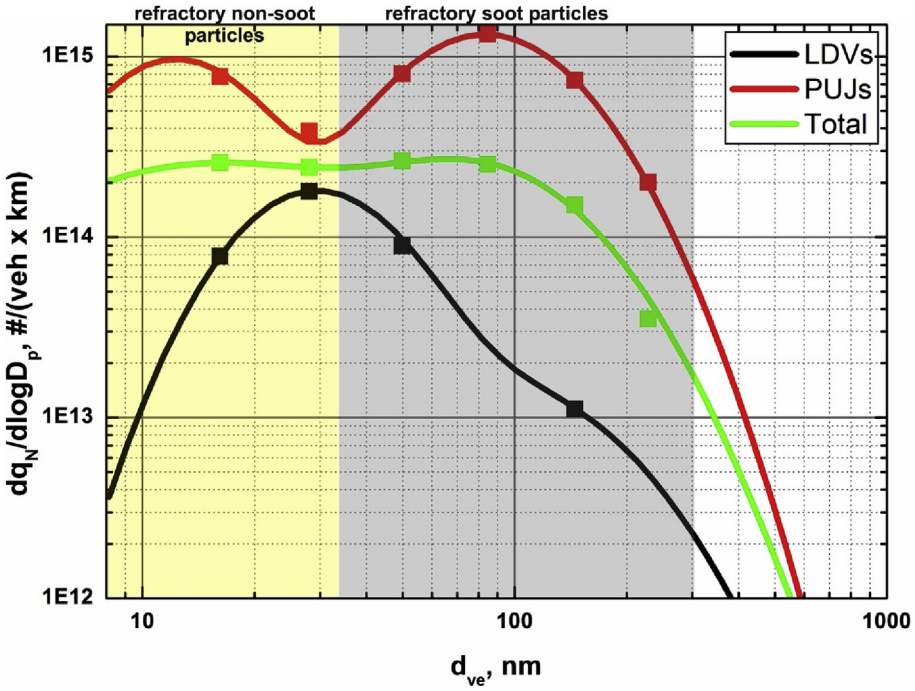

Fig. 9. Size segregated refractory non-soot (yellow shade) and soot (grey shade) particle number emission factors of different vehicular fleets.

was found to be at least one order of magnitude lower than smaller particle (<80 nm). This can be explained as follows: LDVs in Metro Manila is a mixture of diesel and gasoline powered cars, however, the fraction of gasoline cars is much higher. As the diesel vehicle fraction is lower, so was the emission of bigger (>80 nm) soot particles. Conversely, a higher fraction of gasoline powered vehicles in Metro Manila LDVs' fleet determined the dominant refractory particle emission in the 30–80 nm size range. The smaller particles in LDVs emission (<80 nm) most likely were non-volatile and semi-volatile refractory non-soot particles.

PUJs particle number emission size distribution, on the other hand, was different compared to LDVs and comprised of two pronounced particle number modes at around 15 and 80 nm (Fig. 9). We have already discussed in section 3.2 what species possibly contribute to each of the eminent particle modes. Bigger particle mode (at approx. 80 nm) was also observed by Rose et al. (2006) in a similar study in Germany, however, such pronounced emission of smaller and non-volatile particles from diesel vehicles has not been seen before. To retrieve non-volatile PUJs nucleation mode particle number EFs we have fitted values from Table 4 with a log-normal function (geometric mean diameter of 12 nm and sigma of 1.58). This procedure resulted in a non-volatile nucleation mode particle EF of $4.11 \cdot 10^{14}$ rp/(km·veh). These smallest particles were found to account for approximately 36% of overall PUJs emitted refractory particles in terms of particle number while their contribution to total emitted refractory particle mass was found to be less than 0.2%. Despite their little mass, these smallest particles may have a significant effect on urban air quality in terms of pollution-related adverse health effects.

From the results discussed previously, it can be seen that emission of refractory particle number and mass from PUJs is a serious urban pollution problem in Metro Manila. Despite the fact that these vehicles emit as much as lorry-like trucks in western countries, they neither encounter any stringent, environment sustainable technical requirements, nor are banned from the "green zones" (park, school, university, hospital environments, etc.) and are widely used as a means of public transportation. The need to improve emissions from this particular fleet is obvious and urgent.

3.4. General remarks

3.4.1. Emission factors (EFs)

The comparison between emission factors (EFs) determined in this and other studies can be found in Table 3. Only a sparse amount of studies exist in which EFs of soot particles were estimated. Since, not all studies reported EFs of same measured quantities, in the table we have also included subscripts to indicate whether it was soot, black carbon (BC) or the total particles (no subscript). The closest to our study in terms of the applied measurement techniques is the study by Rose et al. (2006). They found that in Leipzig, Germany, average fleet and LDV EFs of soot particle number was 2.2 and 1.7 times lower (when comparing to total refractory particles) than the values we observed in Metro Manila, respectively. In a study in Berlin, Germany, by Birmili et al. (2009), average fleet soot mode (geometric mean diameter of 71 nm) particle EFs was found to be $7.8 \cdot 10^{13}$ sp/(km·veh) that is 4.2 times lower than the values observed in our study. Comparing EFs that were reported from studies in Germany – Berlin particle number EFs of LDV was found to be 2 times lower than soot particle EFs determined in Leipzig. On the other hand, in yet another study in Germany by Nickel et al. (2013), reported EFs of particle number was closer to the ones observed in Metro Manila. When comparing our soot particle number EFs to those reported from the United States (US), we found that in some cases EFs of LDV was lower in Manila than in the US (e.g. Geller et al., 2005), while Kirchstetter et al. (1999) reported EFs of LDV to be 2.5 times lower in the US than in Manila. All suggesting that some kind of variability exist even within the studies conducted in the same country. Please note that in most of the previous studies the total particle number EFs and not only soot or refractory particle number EFs were reported. The closest match to Manila's carbonaceous particle mass EFs of LDV was found to be China (0.027 g/(km·veh) in both countries, Westerdahl et al., 2009).

It is important to understand that direct comparison between our derived EFs and those reported from other countries must be

Table 3
Europe Union emission regulations for particulate matter (PM) and particle number (PN) for passenger cars and light commercial vehicles with a comparison to emission factors estimated in this study. Subscripts "diesel" and "diesel + gasoline" stands for the corresponding standard of either diesel or diesel and gasoline vehicles, respectively. PM_{refr} and PN_{refr} stands for refractory particle mass and refractory particle number emission factors, respectively. Table was adopted from https://www.dieselnet.com/standards/eu/.

Stage	Date	PM, g/km	PN, #/km
Passenger Cars			
EURO 1	1992	0.14_{diesel}	–
EURO 2	1996	$0.08–0.10_{diesel}$	–
EURO 3	2000	0.05_{diesel}	–
EURO 4	2005	0.025_{diesel}	–
EURO 5-6	2009–2014	$0.005_{diesel+gasoline}$	$6.0 \cdot 10^{11}{}_{diesel+gasoline}$
Light commercial veh. (> 1760 kg)			
EURO 1	1994	0.25_{diesel}	–
EURO 2	1998	$0.17–0.20_{diesel}$	–
EURO 3	2001	0.10_{diesel}	–
EURO 4	2006	0.06_{diesel}	–
EURO 5-6	2010–2015	$0.005_{diesel+gasoline}$	$6.0 \cdot 10^{11}{}_{diesel+gasoline}$
This study	Location	PM, g/km	PN, #/km
LDV	Manila, Philippines	0.027_{refr}	$9.79 \cdot 10^{13}{}_{refr}$
Jeepneys	Manila, Philippines	1.618_{refr}	$1.15 \cdot 10^{15}{}_{refr}$
Average fleet	Manila, Philippines	0.313_{refr}	$3.29 \cdot 10^{14}{}_{refr}$
Other studies			
LDV [a,*]	Beijing, China	0.027_{BC}	$1.60 \cdot 10^{14}$
LDV [b,*]	California, USA	0.0027_{BC}	$2.22 \cdot 10^{14}$
LDV [c,*]	California, USA	0.0031_{BC}	$4.00 \cdot 10^{13}$
LDV [d]	Leipzig, Germany	–	$5.80 \cdot 10^{13}$
LDV [e]	Berlin, Germany	–	$2.40 \cdot 10^{13}$
LDV [f]	Meckenheim, Germany	–	$2.10 \cdot 10^{14}$
HDV [a,*]	Beijing, China	0.513_{BC}	$4.36 \cdot 10^{15}$
HDV [b,*]	California, USA	0.306_{BC}	$3.24 \cdot 10^{15}$
HDV [c,*]	California, USA	0.513_{BC}	$2.49 \cdot 10^{15}$
HDV [d]	Leipzig, Germany	–	$2.50 \cdot 10^{15}$
HDV [e]	Berlin, Germany	–	$2.96 \cdot 10^{15}$
HDV [f]	Meckenheim, Germany	–	$1.18 \cdot 10^{15}$

Refr – only refractory particles.
BC – PM reported as black carbon.
* - EFs reported in g/kg of fuel burnt.
[a] Westerdahl et al. (2009).
[b] Geller et al. (2005).
[c] Kirchstetter et al. (1999).
[d] Rose et al. (2006).
[e] Birmili et al. (2009).
[f] Nickel et al. (2013).

Table 4
Size segregated and normalized refractory particle number emission factor (EFs, $\cdot 10^{14}$) for different vehicular fleets: light duty vehicles (LDVs); public utility *Jeepneys* (PUJ); and emission factor per average vehicle. We were not able to retrieve EFs of LDVs at 85 nm and 229 nm.

d_{ve}	16 nm	28 nm	50 nm	85 nm	145 nm	229 nm
$dq_N/dlogD_p$, #/veh*km						
Light Duty Vehicles (LDVs)	0.782	1.770	0.894	–	0.111	–
Public Utility Jeepneys (PUJs)	7.730	3.860	8.020	13.300	7.360	2.000
Average vehicle	2.580	2.420	2.630	2.520	1.500	0.353

viewed critically due to several reasons. Firstly, EFs depend on the pollutant concentration difference between urban street and background sites (delta *C*, Δ*C*) as described by Eq. (3), thus proper estimation of pollutant increment due to traffic emission is very important. For example, in a study by Rose et al. (2006), they used only one VTDMA-system to determine Δ*C* and thus, the measurements at urban and background sites were accomplished in different time periods. This might result in higher uncertainties when estimating Δ*C*. Secondly, measured particle number concentration greatly depends on the measurement technique and the instrumentation used. Several studies indicated that the higher emission factors for particle number concentration were found when instruments with lower detection limits were used (e.g. Nickel et al., 2013). From a study by Birmili et al. (2009) it is clear that there is a large variability of instruments with different detection limits used to evaluate EFs. Moreover, vehicle speeds for which EFs were estimated also span over a large range of values. It is known that different engine operating regimes (idling, accelerating, stopping etc.) do influence EFs and the comparison between values from different studies becomes even more vague (Karjalainen et al., 2014).

For the reasons mentioned above, the comparison between EFs in different studies must be taken with a grain of salt. Nevertheless, we were able to show that traffic related pollutant emissions in Metro Manila and other low-income countries are/may be far from accepted norms and limits.

3.4.2. Possible errors in estimating soot particle concentration from refractory particle fractions

Finally we would like to discuss how close the retrieved refractory particle number and mass could represent actual soot particles. The retrieval of soot particle number distribution, when VTDMA and MPSS systems are used, is based on the assumption that refractory species at a road side are predominantly soot particles and its constituents (e.g. Rose et al., 2006). This assumption, however, might not be always true due to the fact that not only soot particles remain refractory at 300 °C. For example, fine dust particles, particles from mechanical wear of tires, braking pads, some inorganic salts and non-volatile organic material transported from the background or formed on the site may also form externally mixed mode in particle volatility distribution. These particles then might be misleadingly interpreted as soot particles even though their related health effects could be much different. Although in previous studies (e.g. Rose et al., 2006) this step was neglected, we have conducted s refractory particle mass closure to make sure that our retrieved refractory particle number size distribution is a good proxy for soot particle physical properties. Calculated refractory particle mass size distribution allowed us to obtain refractory particle mass in the size range of 10–800 nm, which we then compared to MAAP measurements (Fig. 10).

From here it can be seen that refractory particle mass concentration derived from $f_{N,LV}$ and equivalent black carbon mass (as soot proxy) directly measured with MAAP is in a reasonable agreement (slope of 0.992 and $R^2 = 0.85$). It is worth reminding that our retrieved refractory particle number size distribution is a superposition of refractory non-soot and refractory soot particle modes (as described in section 3.1). For this reason the calculated refractory particle mass is a product of these two modes. However, as can be seen from Fig. 8, the mass of refractory particles is mostly driven by the larger size mode particles (mainly ultrafine soot at 80 nm), and thus, it is correct to assume that our derived refractory particle mass is a good proxy for soot mass. The closure between retrieved refractory and measured soot particles would also be a useful tool to elucidate the origin of the smallest refractory particles. Unfortunately, this type of closure study was not possible at the time of experiment.

4. Summary and conclusions

In this study, we characterized the traffic emissions from a street canyon at a polluted urban environment in Metro Manila, Philippines, during a time period from 16 May to 11 June 2015. A Volatility Tandem Differential Mobility Analyzer (V-TDMA) was used to measure refractory number fraction of sub-micrometer particles at Taft Avenue by evaporating volatile material at 300 °C temperature. In addition, particle number size distribution (PNSD), equivalent black carbon mass concentration (eBC, as soot proxy) and $PM_{2.5}$ measurements were performed with a Mobility Particle Size Spectrometer (MPSS), Multi-Angle Absorption Photometer (MAAP) and a mini-volume sampler (gravimetric method), respectively. The refractory particle number concentration was then extracted from a combination of the externally mixed particle number fraction and the measured PNSD. Supplementary information on meteorological parameters was collected using an autonomous weather station and a sonic anemometer at the heights of the measurement container and the rooftop of the nearby building, respectively. This data was later used to calculate emission factors (EFs) with Operational Street Pollution Model (OSPM).

Our observed size-segregated number fractions of externally mixed particles were noticeably higher (90% versus 60%) than in other similar studies. Moreover, the highest number fraction of refractory particles was found to be higher than in previous studies (229 versus 80 nm). We assume that this is because variability in engine technologies and/or fuel composition. Another difference to previous studies was that, despite some randomness, we were not able to observe defined diurnal variation of particle volatility

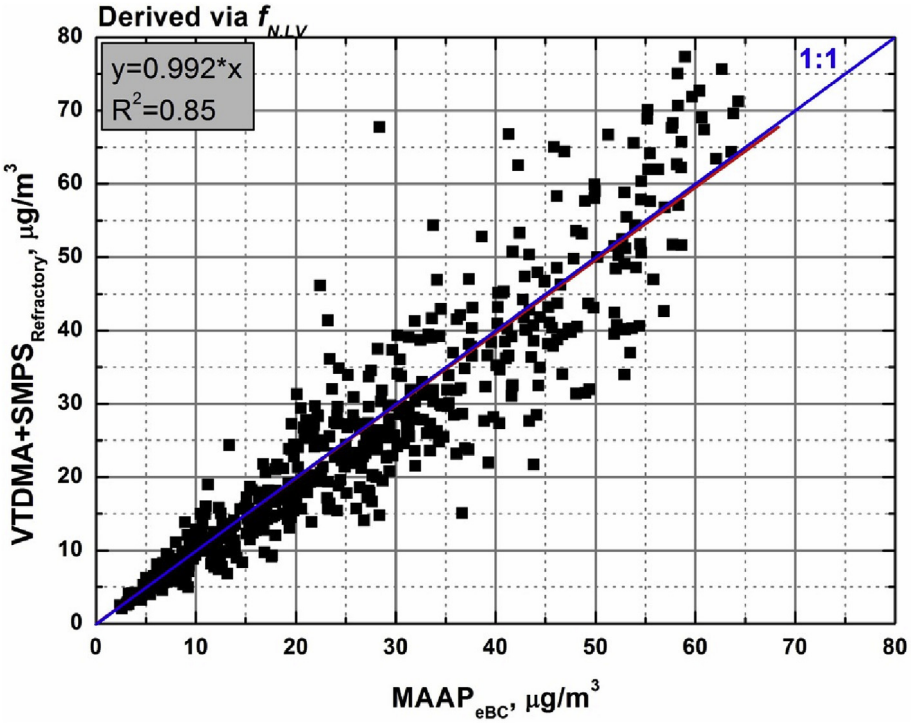

Fig. 10. A Comparison between retrieved refractory particle and measured equivalent black carbon mass concentrations.

properties. The number fractions of refractory species neither followed the diurnal cycle of the traffic, nor it changed when the roadside aerosol was diluted with cleaner air from urban background. These observations suggest that at road side traffic was a dominant pollutant source, which also determined very distinct physical and chemical aerosol particle properties in an urban background environment.

In contrast to refractory number fractions, derived refractory particle number concentration showed a pronounced diurnal cycle, which was found to be the result of both the increase in traffic density and change in local meteorological conditions (wind speed and direction). Refractory particle number concentration reached as high as 15000 particles/cm^3 during morning rush hours and where at least 3 times higher than values reported from western countries. When roadside aerosol was diluted with cleaner background air, refractory particle number concentration decreased to 6000 particles/cm^3. We also found that the World Health Organization limit value for $PM_{2.5}$ was exceeded on all measurement days by an average of 2 fold with refractory particles contributing to total $PM_{2.5}$ from 55 to 75%. Convection-enhanced vertical mixing appeared to be of minor importance in decreasing soot particle number concentration.

The derived refractory particle number size distribution (r-PNSD, soot proxy) was found to be a superposition of two ultrafine modes at 20 and 80 nm. That is noticeably different compared to previous studies, which usually reported only a bigger refractory particle mode. To better understand the origin of nearly nucleation mode particles, we have also calculated size segregated emission factors (EFs) of refractory particles for different vehicle fleets. The separation of the emissions between light duty vehicles (LDVs) and public utility *Jeepneys* (PUJs) led not only to overall higher EFs, but also substantially different shaped EFs size distribution when comparing PUJs and LDVs. While LDVs EFs could be characterized by much stronger mode at around 30 nm and weaker mode at around 100–200 nm, PUJs EF of refractory particles comprised of two, nearly equally strong modes at 10–20 nm and 80–100 nm. The smallest particles were most likely ash from metallic additives in lubricating oil, tiny carbonaceous particles and/or nucleated and oxidized organic polymers, while bigger ones were probably soot agglomerates. Observed extremely high concentrations of smallest particles, which have little to no contribution to particulate mass, may play an important role when assessing health related effects.

Calculated EFs of refractory particle number and mass were $1.15 \cdot 10^{15}$, $9.79 \cdot 10^{13}$ and $3.29 \cdot 10^{14}$ rp/km·veh and 1.618, 0.027 and 0.313 g/km·veh for PUJs, LDVs and average fleet, respectively. The important message from the EFs analysis is that old technology diesel PUJs, being only 20% of total vehicular fleet, contribute up to 75 and 94% of total roadside emitted refractory particle number and soot mass, respectively. It is also worth mentioning that PUJs, not like heavy duty vehicles, do not encounter traffic bans and are able to drive streets of Metro Manila with no restrictions regarding environmental protection. The reduction of PUJs emission by improving fuel quality and engine technology, using particulate filters or banning this type of vehicles from the streets may contribute significantly to the reduction of carbonaceous particulate pollutants in urban Metro Manila. Reinforcement of more stringent environmental legislation and technical requirements are also advisable.

Due to the complexity, such studies are rare in low-income countries and yet are much desired. The unique findings presented here can be used in urban air quality models and health studies as well as to demonstrate that a better indicator to evaluate air quality and possible health related risks than PM_{10} or $PM_{2.5}$ is very much needed. Especially in the developing regions where unsustainable urbanization has led to traffic related pollution problems. Our future work will focus on accessing individual exposure to high levels of ultrafine soot particulates in polluted urban environments.

Acknowledgement

This study was supported by the Partnership for Clean Air Inc., the Researchers for Clean Air, Inc., the Metro Manila Development Authority, the City Office of Manila, De La Salle University (through URCO project number 35FU2TAY11-3TAY12 and the visiting professor grants of the Vice-Chancellor for Academics), CHED (COE research grant of Dr. Vallar and Dr. Galvez) and Leibniz-Institut für Troposphärenforschung e.V. (TROPOS). This study was also supported by the Ministry of Science, ICT and Future Planning in South Korea through the International Environmental Research Center and the UNU & GIST Joint Programme on Science and Technology for Sustainability in 2015. We would also like to acknowledge Mr. Alberto Suansing, Kristine Loise Simangan, Catrina Urbiztondo, Red Castilla, Floyd Rey Plando, Neil Matthew Anore, Kevin Apoloan, Sanmiguel Arkanghel Dichoso, and Sherwin Movilla for their participation in this phase of the campaign.

Appendix A. Supplementary data

Supplementary data related to this article can be found at https://doi.org/10.1016/j.atmosenv.2017.09.037.

References

Abdel-Shafy, H.I., Mansour, M.S., 2016. A review on polycyclic aromatic hydrocarbons: source, environmental impact, effect on human health and remediation. Egypt. J. Petroleum 25 (1), 107–123.
Abu-Allaban, M., Gillies, J.A., Gertler, A.W., Clayton, R., Proffitt, D., 2003. Tailpipe, resuspended road dust, and brake wear emission factors from on-road vehicles. Atmos. Environ. 37, 5283–5293.
Aggarwal, S., Jain, R., Marshall, J.D., 2012. Real-time prediction of size-resolved ultrafine particulate matter on freeways. Environ. Sci. Technol. 46 (4), 2234–2241.
Akasaka, Ikumi, 2010. Interannual variations in seasonal march of rainfall in the Philippines. Int. J. Climatol. 30 (9), 1301–1314.
Berkowicz, R., 2000. OSPM—a parameterised street pollution model. Environ. Monit. Assess. 65, 323–331.
Birmili, W., Alaviippola, B., Hinneburg, D., Knoth, O., Tuch, T., Borken-Kleefeld, J., Schacht, A., 2009. Dispersion of traffic-related exhaust particles near the Berlin urban motorway–estimation of fleet emission factors. Atmos. Chem. Phys. 9 (7), 2355–2374.
Braganza, A., Liwanag, A., Palines, C., 2007. Comparison of Local Jeepney Specification and Selected Philippine National Standards for Road Vehicles. University of the Philippines Diliman, Quezon City.
Brizio, E., Genon, G., Borsarelli, S., 2007. PM emissions in a urban context. Am. J. Environ. Sci. 3, 166.
Brown, D., Wilson, M., MacNee, W., Stone, V., Donaldson, K., 2001. Size-dependent proinflammatory effects of ultrafine polystyrene particles: a role for surface area and oxidative stress in the enhanced activity of ultrafines. Toxicol. Appl. Pharmacol. 175 (3), 191–199.
Burtscher, H., Baltensperger, U., Bukowiecki, N., Cohn, P., Hüglin, C., Mohr, M., Matter, U., Nyeki, S., Schmatloch, V., Streit, N., Weingartner, E., 2001. Separation of volatile and non-volatile aerosol fractions by thermodesorption: instrumental development and applications. J. Aerosol Sci. 32 (4), 427–442.
Engler, C., Rose, D., Wehner, B., Wiedensohler, A., Brüggemann, E., Gnauk, T., Spindler, G., Tuch, T., Birmili, W., 2007. Size distributions of non-volatile particle residuals (Dp< 800 nm) at a rural site in Germany and relation to air mass origin. Atmos. Chem. Phys. 7 (22), 5785–5802.
Floater, G., Rode, P., Slavcheva, R., Hoornweg, D., Kennedy, C., Robert, A., 2014. Cities and the New Climate Economy: the Transformative Role of Global Urban Growth—paper 1. NCE Cities. LSE cities —London School of Economics and Political Science, London.
Geller, M.D., Sardar, S.B., Phuleria, H., Fine, P.M., Sioutas, C., 2005. Measurements of particle number and mass concentrations and size distributions in a tunnel environment. Environ. Sci. Technol. 39 (22), 8653–8663.
Gurjar, B.R., Butler, T.M., Lawrence, M.G., Lelieveld, J., 2008. Evaluation of emissions and air quality in megacities. Atmos. Environ. 42 (7), 1593–1606.
Gurjar, B.R., Jain, A., Sharma, A., Agarwal, A., Gupta, P., Nagpure, A.S., Lelieveld, J., 2010. Human health risks in megacities due to air pollution. Atmos. Environ. 44 (36), 4606–4613.
Gysel, M., McFiggans, G.B., Coe, H., 2009. Inversion of tandem differential mobility analyser (TDMA) measurements. J. Aerosol Sci. 40 (2), 134–151.

Heyder, J., Gebhart, J., Rudolf, G., Schiller, C.F., Stahlhofen, W., 1986. Deposition of particles in the human respiratory tract in the size range 0.005–15 μm. J. Aerosol Sci. 17 (5), 811–825. https://doi.org/10.1016/0021-8502(86)90035-2.

Ibald-Mulli, A., Wichmann, H.E., Kreyling, W., Peters, A., 2002. Epidemiological evidence on health effects of ultrafine particles. J. Aerosol Med. 15 (2), 189–201.

Janssen, N.A., Hoek, G., Simic-Lawson, M., Fischer, P., Van Bree, L., Ten Brink, H., Keuken, M., Atkinson, R.W., Anderson, H.R., Brunekreef, B., Cassee, F.R., 2011. Black carbon as an additional indicator of the adverse health effects of airborne particles compared with PM˙ sub 10˙ and PM˙ sub 2.5˙. Environ. health Perspect. 119 (12), 1691.

Kakosimos, K.E., Hertel, O., Ketzel, M., Berkowicz, R., 2010. Operational Street Pollution Model (OSPM) – a review of performed application and validation studies, and future prospects. Environ. Chem. 7 (6), 485–503.

Karjalainen, P., Pirjola, L., Heikkilä, J., Lähde, T., Tzamkiozis, T., Ntziachristos, L., Keskinen, J., Rönkkö, T., 2014. Exhaust particles of modern gasoline vehicles: a laboratory and an on-road study. Atmos. Environ. 97, 262–270.

Kecorius, S., Tamayo, E.G., Galvez, M.C., Madueño, L., Betito, G., Gonzaga-Cayetano, M., Vallar, E., Wiedensohler, A., 2017. Time Spent in Micro-environments by University Occupants and Their Family Members in Metro Manila – Philippines (in preparation).

Kittelson, D., Kraft, M., 2014. Particle Formation and Models in Internal Combustion Engines. University of Cambridge, United Kingdom.

Kirchstetter, T.W., Harley, R.A., Kreisberg, N.M., Stolzenburg, M.R., Hering, S.V., 1999. On-road measurement of fine particle and nitrogen oxide emissions from light- and heavy-duty motor vehicles. Atmos. Environ. 33 (18), 2955–2968.

Knudsen, J.N., Jensen, P.A., Johansen, D.K., 2004. Transformation and release to the gas phase of Cl, K, and S during combustion of annual biomass. Energy Fuels 18 (5), 1385–1399.

Laudico, A.V., Mirasol-Lumague, M.R., Mapua, C.A., Uy, G.B., Toral, J.A.B., Medina, V.M., Pukkala, E., 2010. Cancer incidence and survival in Metro Manila and rizal province, Philippines. Jpn. J. Clin. Oncol. 40 (7), 603–612.

Marco, G., Bo, X., 2013. Air quality legislation and standards in the European Union: background, status and public participation. Adv. Clim. Change Res. 4 (1), 50–59.

Mills, N.L., Robinson, S.D., Fokkens, P.H., Leseman, D.L., Miller, M.R., Anderson, D., Freney, E.J., Heal, M.R., Donovan, R.J., Blomberg, A., Sandström, T., 2008. Exposure to concentrated ambient particles does not affect vascular function in patients with coronary heart disease. Environ. health Perspect. 116 (6), 709.

Müller, T., Schladitz, A., Massling, A., Kaaden, N., Kandler, K., Wiedensohler, A., 2009. Spectral absorption coefficients and imaginary parts of refractive indices of Saharan dust during SAMUM-1. Tellus B 61, 79–95.

Nickel, C., Kaminski, H., Hellack, B., Quass, U., John, A., Klemm, O., Kuhlbusch, T.A., 2013. Size resolved particle number emission factors of motorway traffic differentiated between heavy and light duty vehicles. Res 13, 450–461.

Ning, Z., Chan, K.L., Wong, K.C., Westerdahl, D., Močnik, G., Zhou, J.H., Cheung, C.S., 2013. Black carbon mass size distributions of diesel exhaust and urban aerosols measured using differential mobility analyzer in tandem with Aethalometer. Atmos. Environ. 80, 31–40.

Oanh, N.K., Upadhyay, N., Zhuang, Y.H., Hao, Z.P., Murthy, D.V.S., Lestari, P., Villarin, J.T., Chengchua, K., Co, H.X., Dung, N.T., Lindgren, E.S., 2006. Particulate air pollution in six Asian cities: spatial and temporal distributions, and associated sources. Atmos. Environ. 40 (18), 3367–3380.

Palmgren, F., Berkowicz, R., Ziv, A., Hertel, O., 1999. Actual car fleet emissions estimated from urban air quality measurements and street pollution models. Sci. Total Environ. 235 (1), 101–109.

Park, K., Kittelson, D.B., McMurry, P.H., 2004. Structural properties of diesel exhaust particles measured by transmission electron microscopy (TEM): relationships to particle mass and mobility. Aerosol Sci. Technol. 38 (9), 881–889.

Peters, A., Von Klot, S., Heier, M., Trentinaglia, I., Hörmann, A., Wichmann, H.E., Löwel, H., 2004. Exposure to traffic and the onset of myocardial infarction. N. Engl. J. Med. 351 (17), 1721–1730.

Petzold, A., Schönlinner, M., 2004. The Multi-angle absorption photometer – a new method for the measurement of aerosol light absorption and atmospheric black carbon. J. Aerosol Sci. 35, 421–441.

Pfeifer, S., Birmili, W., Schladitz, A., Müller, T., Nowak, A., Wiedensohler, A., 2014. A fast and easy-to-implement inversion algorithm for mobility particle size spectrometers considering particle number size distribution information outside of the detection range. Atmos. Meas. Tech. 7, 95–105. https://doi.org/10.5194/amt-7-95-2014.

Philippin, S., Wiedensohler, A., Stratmann, F., 2004. Measurements of non-volatile fractions of pollution aerosols with an eight-tube volatility tandem differential mobility analyzer (VTDMA-8). J. Aerosol Sci. 35, 185–203.

Pope III, C.A., Dockery, D.W., 2006. Health effects of fine particulate air pollution: lines that connect. J. Air Waste Manag. Assoc. 56, 709–742.

Poulain, L., Birmili, W., Canonaco, F., Crippa, M., Wu, Z.J., Nordmann, S., Spindler, G., Prévôt, A.S.H., Wiedensohler, A., Herrmann, H., 2014. Chemical mass balance of 300 °C non-volatile particles at the tropospheric research site Melpitz, Germany. Atmos. Chem. Phys. 14, 10145–10162. https://doi.org/10.5194/acp-14-10145-2014.

Rader, D.J., McMurry, P.H., 1986. Application of the tandem differential mobility analyzer to studies of droplet growth or evaporation. J. Aerosol Sci. 17 (5), 771–787.

Rose, D., Wehner, B., Ketzel, M., Engler, C., Voigtländer, J., Tuch, T., Wiedensohler, A., 2006. Atmospheric number size distributions of soot particles and estimation of emission factors. Atmos. Chem. Phys. 6 (4), 1021–1031.

Strak, M., Boogaard, H., Meliefste, K., Oldenwening, M., Zuurbier, M., Brunekreef, B., Hoek, G., 2010. Respiratory health effects of ultrafine and fine particle exposure in cyclists. Occup. Environ. Med. 67 (2), 118–124.

Sun, H., Biedermann, L., Bond, T., 2007. Color of brown carbon: a model for ultraviolet and visible light absorption by organic carbon aerosol. Geophys. Res. Lett. 34 (17), L17813.

Thorpe, A., Harrison, R.M., 2008. Sources and properties of non-exhaust particulate matter from road traffic: a review. Sci. Total Environ. 400 (1), 270–282.

Tiitta, P., Miettinen, P., Vaattovaara, P., Joutsensaari, J., Petäjä, T., Virtanen, A., Raatikainen, T., Aalto, P., Portin, H., Romakkaniemi, S., Kokkola, H., 2010. Roadside aerosol study using hygroscopic, organic and volatility TDMAs: characterization and mixing state. Atmos. Environ. 44 (7), 976–986.

Tuch, T.M., Haudek, A., Müller, T., Nowak, A., Wex, H., Wiedensohler, A., 2009. Design and performance of an automatic regenerating adsorption aerosol dryer for continuous operation at monitoring sites. Atmos. Meas. Tech. 2, 417–422. https://doi.org/10.5194/amt-2-417-2009.

Vergel, K.B., Tiglao, N.C.C., 2013. Estimation of emissions and fuel consumption of sustainable transport measures in Metro Manila. Philipp. Eng. J. 34 (1).

Villafuerte, M.Q., Matsumoto, J., Akasaka, I., Takahashi, H.G., Kubota, H., Cinco, T.A., 2014. Long-term trends and variability of rainfall extremes in the Philippines. Atmos. Res. 137, 1–13.

Vinzents, P.S., Møller, P., Sørensen, M., Knudsen, L.E., Hertel, O., Jensen, F.P., Schibye, B., Loft, S., 2005. Personal exposure to ultrafine particles and oxidative DNA damage. Environ. Health Perspect. 1485–1490.

Wehner, B., Philippin, S., Wiedensohler, A., Scheer, V., Vogt, R., 2004. Variability of non-volatile fractions of atmospheric aerosol particles with traffic influence. Atmos. Environ. 38 (36), 6081–6090.

Westerdahl, D., Wang, X., Pan, X., Zhang, K.M., 2009. Characterization of on-road vehicle emission factors and microenvironmental air quality in Beijing, China. Atmos. Environ. 43 (3), 697–705.

Wiedensohler, A., Orsini, D., Covert, D.S., Coffmann, D., Cantrell, W., Havlicek, M., Brechtel, F.J., Russell, L.M., Weber, R.J., Gras, J., Hudson, J.G., 1997. Intercomparison study of the size-dependent counting efficiency of 26 condensation particle counters. Aerosol Sci. Technol. 27 (2), 224–242.

Wiedensohler, A., Birmili, W., Nowak, A., Sonntag, A., Weinhold, K., Merkel, M., Wehner, B., Tuch, T., Pfeifer, S., Fiebig, M., Fjäraa, A.M., Asmi, E., Sellegri, K., Depuy, R., Venzac, H., Villani, P., Laj, P., Aalto, P., Ogren, J.A., Swietlicki, E., Williams, P., Roldin, P., Quincey, P., Hüglin, C., Fierz-Schmidhauser, R., Gysel, M., Weingartner, E., Riccobono, F., Santos, S., Grüning, C., Faloon, K., Beddows, D., Harrison, R., Monahan, C., Jennings, S.G., O'Dowd, C.D., Marinoni, A., Horn, H.-G., Keck, L., Jiang, J., Scheckman, J., McMurry, P.H., Deng, Z., Zhao, C.S., Moerman, M., Henzing, B., de Leeuw, G., Löschau, G., Bastian, S., 2012. Mobility particle size spectrometers: harmonization of technical standards and data structure to facilitate high quality long-term observations of atmospheric particle number size distributions. Atmos. Meas. Tech. 5, 657–685. https://doi.org/10.5194/amt-5-657-2012.

Zhang, Y.L., Cao, F., 2015. Fine particulate matter (PM2.5) in China at a city level. Sci. Rep. 5, 14884.

Zhu, T., Melamed, M.L., Parrish, D., Gauss, M., Klenner, L.G., Lawrence, M.G., Konare, A., Lioussse, C., 2012. WMO/IGAC Impacts of Megacities on Air Pollution and Climate; GAW Report No. 205. World Meteorological Organization (WMO)/International Global Atmospheric Chemistry (IGAC), Geneva, Switzerland (Accessed Feb 03 2017). http://www.wmo.int/pages/prog/arep/gaw/documents/Final_GAW_205.pdf.